View metadata, citation and similar papers at core.ac.uk

brought to you by CORE

provided by Nottingham ePrints

The University of Nottingham

UNITED KINGDOM · CHINA · MALAYSIA

Guillerna, A. Bilbao and Axinte, D.A. and Billingham, John (2015) The linear inverse problem in energy beam processing with an application to abrasive waterjet machining. International Journal of Machine Tools & Manufacture, 99 . pp. 34-42. ISSN 0890-6955

Access from the University of Nottingham repository:
http://eprints.nottingham.ac.uk/34680/2/linear_inverse.pdf

Copyright and reuse:

The Nottingham ePrints service makes this work by researchers of the University of Nottingham available open access under the following conditions.

This article is made available under the Creative Commons Attribution Non-commercial No Derivatives licence and may be reused according to the conditions of the licence. For more details see: http://creativecommons.org/licenses/by-nc-nd/2.5/

A note on versions:

The version presented here may differ from the published version or from the version of record. If you wish to cite this item you are advised to consult the publisher's version. Please see the repository url above for details on accessing the published version and note that access may require a subscription.

For more information, please contact eprints@nottingham.ac.uk

International Journal of Machine Tools & Manufacture 99 (2015) 34–42

Contents lists available at ScienceDirect

International Journal of Machine Tools & Manufacture

journal homepage: www.elsevier.com/locate/ijmactool

The linear inverse problem in energy beam processing with an application to abrasive waterjet machining

A. Bilbao Guillerna [a], D. Axinte [a,*], J. Billingham [b]

[a] Machining and Condition Monitoring Group, Faculty of Engineering, The University of Nottingham University Park, NG7 2RD, UK
[b] School of Mathematical Sciences, The University of Nottingham University Park, NG7 2RD, UK

ARTICLE INFO

Article history:
Received 17 April 2015
Received in revised form
2 September 2015
Accepted 2 September 2015
Available online 10 September 2015

Keywords:
Inverse problem
Controlled depth etching
Energy beam
Abrasive waterjet machining

ABSTRACT

The linear inverse problem for energy beam processing, in which a desired etched profile is known and a trajectory of the beam that will create it must be found, is studied in this paper. As an example, abrasive waterjet machining (AWJM) is considered here supported by extensive experimental investigations. The behaviour of this process can be described using a linear model when the angle between the jet and the surface is approximately constant during the process, as occurs for shallow etched profiles. The inverse problem is usually solved by simply controlling dwell time in proportion to the required depth of milling, without considering whether the target surface can actually be etched. To address this, a Fourier analysis Is used to show that high frequency components in the target surface cannot be etched due to the geometry of the jet and the dynamics of the machine. In this paper, this frequency domain analysis is used to improve the choice of the target profile in such a way that it can be etched. The dynamics of the machine also have a large influence on the actual movement of the jet. It is very difficult to describe this effect because the controller of the machine is usually unknown. A simple approximation is used for the choice of the slope of a step profile. The tracking error between the desired trajectory and the real one is reduced and the etched profile is improved. Several experimental tests are presented to show the usefulness of this approach. Finally, the limitations of the linear model are studied.

© 2015 The Authors. Published by Elsevier Ltd. This is an open access article under the CC BY-NC-ND license (http://creativecommons.org/licenses/by-nc-nd/4.0/).

1. Introduction

Abrasive Waterjet Machining (AWJ) machining is a fast-growing non-conventional technology capable of processing any material regardless of its properties. Modern AWJ machining systems make use of high-pressure water jets (up to 90 000 psi = 620 MPa) forced through a tiny orifice (0.1–0.3 mm) that enables the entrainment and acceleration of abrasive particles (e.g. garnet, Al2O3) to high velocities (200–800 m/s). When the resulting three-phase jet plume (water, abrasives and air, [1]) impacts a target surface, it removes material by abrasive erosion (i.e. erosion by solid particle impingement) [2–4].

The inverse problem consists of defining the control parameters, in particular the 3D beam path (position and orientation of the beam as a function of time), to create a prescribed freeform surface. This inverse problem is well understood for conventional machining (e.g. turning, grinding, drilling), because the cutting tool geometry is well defined and the material removal is a *time independent process*. In contrast, energy beam (EB) machining is achieved through the local interaction of an energy beam of particular characteristics (e.g. energy distribution), which leads to a time-dependent removal rate. Furthermore, EB machining is a time-dependent process in which not only does the etched surface vary with the dwell time, but also any acceleration or deceleration of the machine/beam delivery system when performing raster paths will influence the actual geometry of the surface generated. This makes the process inherently nonlinear, and dependent upon good mathematical models, which then have to be inverted to produce a suitable beam path, i.e. solving the inverse problem.

Some research in addressing the direct problem, i.e. given a model for the footprint and the beam path, to determine the generated surface, has been reported. Some of the most common methods are based on statistical approaches [5], finite element methods [6–8] or artificial intelligence methods [9]. Finite element methods have also been used to model overlapped footprints [10]. However, there are some important drawbacks to these three methods: statistical methods are only valid if the operating parameters are near the ones used for the modelling; finite element approaches are computationally expensive and simplifying hypotheses are needed; artificial intelligence approaches requires significant sets of data for training and give little insight into the details of the physics that affect the process.

There is another set of more thorough approaches for

* Corresponding author.

http://dx.doi.org/10.1016/j.ijmachtools.2015.09.006
0890-6955/© 2015 The Authors. Published by Elsevier Ltd. This is an open access article under the CC BY-NC-ND license (http://creativecommons.org/licenses/by-nc-nd/4.0/).

predicting footprint profiles based on analytical/geometric modelling. One of the first studies details a model of the footprints of stationary air powder-blaster jets [11]. The advantage of such models is their relationship to the physical process of material removal and their ability to predict the jet footprint whenever the initial conditions are known [12]. This approach has been mainly used for the prediction of single trenches when the jet impingement angle is $\pi/2$ rad and the path used is straight [13]. Recently, some studies have been published that consider free-moving trajectories of the jet [14] and the effect of the overlapping of raster paths [15].

In contrast, the inverse problem in EB controlled-depth machining, the more technically important and yet academically challenging problem, has not been studied in detail. The most common strategy is simply to vary the dwell time of the beam on each pixel of the target surface [16]. This is simply the leading order approximation to the necessary strategy when the radius of the beam is small compared to the size of the feature that is being etched. There has been some work on the inverse problem for other time-dependent processes: electro-chemical machining [17], where the tool/electrode works in tangential mode to envelope the required surface and is more similar to the movement of a cam than to the energy beam inverse problem; electro-discharge machining [18] where the electrode, with wear pattern measured at time intervals, copies the geometry of the final surface, so a mathematical solution to the inverse problem is not required.

In this paper a new approach to the inverse problem for EB processes, with an emphasis on abrasive Waterjet Machining (AWJM) is presented. Most of the previous solutions just consist of varying the dwell time in proportion to the required depth of milling to achieve the desired surface. However, they do not consider whether a solution to the inverse problem actually exists. In other words, the target surface is usually defined without checking whether the process can etch that particular surface. We will show below that some frequency components, usually high frequency ones, cannot be etched due to the geometry of the jet. A Fourier analysis can be used to find a solution to this problem. This approach gives information about what kind of surfaces can be etched by checking the influence of each frequency on the etched surface. Moreover, an exact solution to the problem can be calculated. The dynamics of the machine also have a large influence on the actual trajectory of the energy beam. Developing an understanding of and a model for these dynamics is difficult, because most of the control parameters of the machine are not accessible to the user. However, for some particular profiles the machine dynamics can be compensated. In [19], the slope of a ramp on the target surface is calculated using the maximum value of the jerk that the AWJM can achieve. This seems to be the first approach to consider the dynamics of the machine tool when precise surfaces are required in EB machining and further analysis is needed for more complicated surfaces where the behaviour of the machine changes during the trajectory. However, this approach is good enough to select the appropriate value of the slope of a ramp. The tracking error between the desired trajectory and the target one is reduced and the quality of the etched surface is improved.

1.1. Scope of the paper

The inverse problem is studied for a general EB process, with particular emphasis on its application to AWJ machining. To achieve this scope the following aspects have been investigated:

1. For shallow surfaces a linear model describes the process well, and a frequency domain analysis can be performed to obtain the solution of the inverse problem. This approach gives information about what kind of surfaces can be etched.
2. The machine dynamics are compensated when a step is included in the target surface; the maximum value of the jerk is measured and used to decide the slope of the ramp.
3. Experimental results indicate when a linear model is valid and when a nonlinear model is needed. Different values of the depths for the target profile are considered and the influence of overlapping between two consecutive passes of the energy beam is studied.

2. Generic model of an energy beam process

A generic partial differential equation model for an energy beam process is

$$\frac{\partial Z}{\partial t} = -E_0(\boldsymbol{x}, t, Z, \nabla Z; \boldsymbol{a}, \boldsymbol{p}(t)), \tag{1}$$

subject to $Z(\boldsymbol{x}, 0) = Z_0(\boldsymbol{x})$. In this model, E_0 is the etching rate function, which characterises the rate of removal of material, t is time, with $0 \le t \le T$, $\boldsymbol{x}=(x, y)$ is spatial position, $z = Z(\boldsymbol{x}, t)$ is the evolving position of the surface in a Cartesian coordinate system, (x, y, z). In addition, $\boldsymbol{a}$ is a vector of constant parameters that characterize the model and $\boldsymbol{p}(t)$ is a vector of control parameters. The appearance of Z and ∇Z in E_0 indicates that, in general, the slope of the evolving surface and its distance from the nozzle affect the rate at which material is removed. In the forward problem, the final surface, $Z(\boldsymbol{x}, T)$, is determined by the choice of control parameters, $\boldsymbol{p}$(t). In the inverse problem, the objective is to find $\boldsymbol{p}$ (t) given a specified target surface, $Z(\boldsymbol{x}, T)$.

In this paper, it is assumed that the initial surface is flat ($Z_0(\boldsymbol{x})=0$) and the linearized problem is studied. In the context of AWJM (Fig. 1), upon which this paper focuses, this means that the feed speed is assumed to be sufficiently high that nonlinear effects due to the evolving slope of the surface and its distance from the nozzle can be neglected, an assumption that can be tested experimentally. In this case, (1) can be written as the linear equation.

$$\frac{\partial Z}{\partial t} = -E_0(\boldsymbol{x}, t, 0, 0; \boldsymbol{a}, \boldsymbol{p}(t)). \tag{2}$$

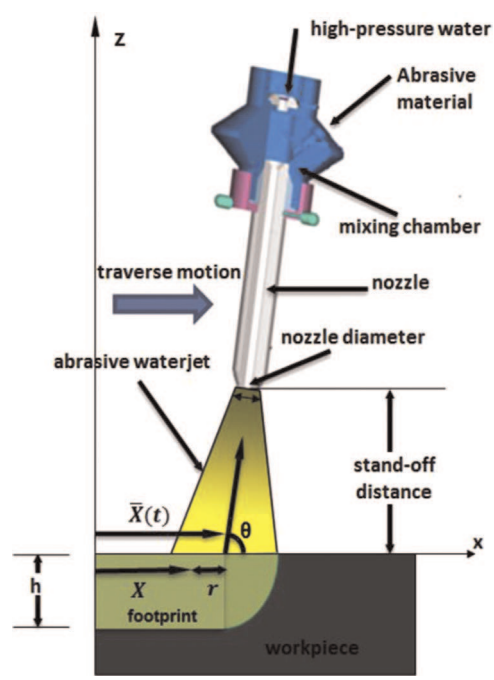

Fig. 1. AWJM model.

In order to make some analytical progress and easily compare theory to experiment, we will further restrict our attention to the case where the axis of the AWJ plume remains perpendicular to the plane, z=0, of the unetched surface, so that

$$\frac{\partial Z}{\partial t} = -E(r), \tag{3}$$

where $r = |\boldsymbol{x} - \boldsymbol{X}(t)|$ is the distance to the centre of the beam, $\boldsymbol{X}(t)$, projected onto $z = 0$, which provides the only control parameters, and $E(r)$ is the etching rate function.

As described in Kong et al. (2012) $E(r)$, can be calibrated experimentally by using a jet with high feed speed to generate a straight, shallow trench, from which $E(r)$ can be calculated using

$$E(r) = \frac{1}{\pi}\left[\int_r^1 s\frac{\left(Z_f(s) - Z_f(r)\right)}{\left(s^2 - r^2\right)^{\frac{3}{2}}}ds - \frac{Z_f(r)}{\sqrt{1 - r^2}}\right]. \tag{4}$$

Here $Z_f(y)$ is the measured profile across the trench and distance is measured in units of beam radius.

3. Linear inverse problem

In the inverse problem the objective is to find the appropriate values of the control parameters, in this case $\boldsymbol{X}(t)$, to obtain a final surface close to a given target surface. For a nonlinear model of the form given by (1), this is a complex optimization problem that requires significant computational resources and will be the subject of a future paper. By studying the linearized inverse problem, using Eq. (3), significant insight can be gained into some fundamental limitations on the family of surfaces that can be etched using a beam with a given footprint, $E(r)$. It also gives a simple framework within which to study the influence of the dynamics of the machine, which experimental tests show to be very significant.

The experimental tests discussed in Section 4 are all for straight paths etched by a jet with a variable feed speed, which results in straight trenches of variable depth. The centreline of these trenches can be treated as the outcome of a one-dimensional etching process. The centreline of these trenches can be treated as the outcome of a one-dimensional etching process. We therefore consider (3) in 1D, so that

$$\frac{\partial Z}{\partial t} = -E(x - X(t)), \tag{5}$$

where x is position along the trench, $X(t)$ is the position of the centre of the jet and E is the etching rate function, assumed to be an even function of its argument, obtained using the experimental calibration procedure described above. The final etched surface is

$$Z(x,\ T) = -\int_0^T E(x - X(t))dt. \tag{6}$$

If we also assume that $X(t)$ is strictly increasing (the jet never retraces its path),[1] we can write (6) as

$$Z(x,\ T) = -\int_{-L}^{L} E\left(x - X(x')\right)D(x')dx', \tag{7}$$

where $D(x) \equiv (\frac{dX}{dt})^{-1}$ is the dwell time as a function of position along the path, which runs from $x = -L$ to $x = L$. Then, by the convolution theorem,

$$Z_n = -2LE_nD_n, \tag{8}$$

where

$$E_n = \frac{1}{2L}\int_{-L}^{L} E(x)e^{-in\pi x/L}dx, \tag{9}$$

is the nth Fourier component of $E(x)$ and similarly for Z_n and D_n.[2]

Since E_n can be calculated from the calibrated etching rate function, $E(x)$, as can Z_n from a given target trench depth profile, $Z(x, T)$, in principle D_n, and hence the required dwell time profile, $D(x)$, can be calculated. However, if E_n=0 for some n, then that mode has no effect on the etched surface. Moreover, if some E_n is small but nonzero (as is typical for high order modes of the Fourier transform of a function with finite support) it will lead to a correspondingly large value of D_n. It can be concluded that, not only is there a fundamental restriction on the frequency content of the final target surface that comes from the frequency content of the etching rate function, but also that, if a given frequency does exist in $E(x)$ but is small, it induces a correspondingly large component in the dwell time, $D(x)$, and hence in the beam path, $X(t)$, that may not be realizable in practice due to the dynamics of the AWJ machine, which is discussed below.

4. Compensation of the dynamics of the machine

The dynamics of the machine have a big influence on the possible movement of the jet. Although the trajectory of the jet is usually implemented as a CNC file, the controller used by the machine to generate the actual trajectory is usually unknown and the identification of a model valid under any conditions is not an easy task. For example, if a step is defined as in Fig. 2(a), where the slope is determined by Z_1, Z_2 and ΔX, then the required feed speed, calculated using the linear model (3), is shown in Fig. 2(b). In this paper two different approaches are used to compensate for the dynamics of the machine when a step like this is implemented in the required trajectory.

4.1. Frequency analysis approach

For a particular step the jet trajectory is calculated and implemented in the machine, and then the actual trajectory is measured. The input and measured trajectories are then compared in the frequency domain. A Frequency Response Function (FRF) can be calculated from those signals. For any other step the trajectory can be compensated by multiplying by the inverse of the FRF in the frequency domain. From (8),

$$Z_n = -2LE_nD_nH_n, \tag{10}$$

where H_n is the FRF calculated as

$$H_n = \frac{\bar{X}_n^{measured}}{\bar{X}_n^{input}}, \tag{11}$$

where $\bar{X}_n^{measured}$ and $\bar{X}_n^{input}$ are the measured and input trajectories of the beam in the frequency domain. Similar conclusions as in Section 3 can be reached in this case with the inclusion of this FRF. If the value of H_n is zero for a particular mode, that frequency cannot appear on the etched surface since it is filtered by the dynamics of the machine. The main advantage of this method is that one can know the range of frequencies that can be included in

[1] This assumption is not restrictive as a path that reverses its direction can be replaced with an equivalent unidirectional path within the context of a linear theory.

[2] The theory is presented in terms of a periodic extension of the path and a Fourier series. It could equally well have been derived using a Fourier transform. Once the transformations are implemented numerically as discrete versions, the results are equivalent.

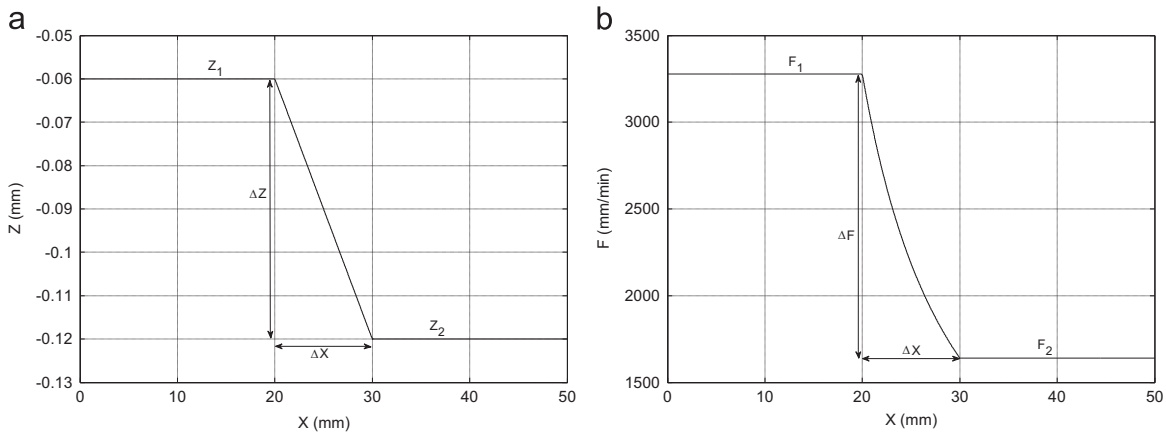

Fig. 2. Definition of a step in the target surface (a) and the calculated feed speed of the machine (b).

the target surface. However, although this is a convenient framework within which to understand how the dynamics of the machine affect the range of surfaces that can be etched, these dynamics are unavoidably nonlinear. In the experimental tests we therefore used a different approach to compensate the machine dynamics.

4.2. Maximum gradient approach

In this method different values of Δx are considered for a particular step (Fig. 2) with constant values for Z_1 and Z_2. For each value of Δx the response is measured and the value of the gradient of the feed speed, $F(x)$, is calculated in the middle of the step.[3] For small values of the slope the machine is able to achieve the desired gradient. However, when the gradient is too large it cannot be obtained.

In order to compensate for the dynamics the following steps are taken:

1. Define the desired value of the slope (s) for the step in the profile and calculate the gradient of $F(x)$ in the middle of the step using

$$s = -KF_m^{-2}G(F_m) \tag{12}$$

   where $F_m=(F_1+F_2)/2$ is the mean value of the feed speed and $G(F_m)$ is the value of the gradient in the middle of the step. $F_1$and F_2 are the values of the feed speed needed to obtain the target depths, Z_1 and Z_2. K is a constant parameter obtained for experimental data.
2. Use the measured data to calculate the value of Δx that gives the desired value of the gradient obtained in the previous step.
3. Compensate the look-ahead option of the machine by changing the position of the step. The controller of the machine calculates the trajectory by considering the next points in the commanded input. For this reason the jet starts accelerating or decelerating in a different position. This value is unknown, but it can be compensated if the position of the step is moved.
4. Use round corners to avoid the high frequency components that are identified as being impossible to etch using the theoretical results given above.
5. Generate the new target profile with those values and calculate the input trajectory using (8). Since the gradient depends on the sign of $\Delta F=F_2-F_1$, the etching is always done in one direction (no raster paths)

[3] Note that the spatial gradient of the feed speed, $F(x)$, is the acceleration divided by the feed speed.

The proposed method can be summarized as the following steps:

1. First, an experimental shallow trench Is generated to calibrate the linear model described in Eq. (3). the etching rate function, $E(r)$, Is calculated using Eq. (4)
2. The small frequency components in the etching rate function are avoided in the target surface. in particular, High frequencies are not included in the target surface.
3. The trajectory of the beam Is obtained from the inverse of the Fourier transform of the dwell time, D_n, calculated using Eq. (8).
4. Finally, the dynamics of the machine are compensated using the method described in Section 4.

5. Experimental tests

The experimental data for model validation has been generated with a Microwaterjet 3-axis F4 type machine developed by Waterjet AG[4] (Fig. 3). Several cutting heads, with a diameter of the mixing nozzle from 0.2 to 0.8 mm, can be mounted in the system. The diameter of the water orifice varies from 0.08 to 0.24 mm. The machine is empowered by a KMT streamline SL-V100D ultra-high pressure pump, capable of delivering a pressure range from 700 to 4000 bar. The apparatus has been designed for high accuracy cutting applications, with a cutting accuracy of 0.01 mm and a positioning accuracy of 0.003 mm, and its maximum traverse speed is 4000 mm/s. The abrasive particles used for this study are BARTON HPX 220. The following constant parameters are considered: $P=138$ MPa, $m_a=0.03$ kg/min, SOD (stand-off distance)= 3 mm. The diameters of the mixing and water nozzles are 0.5 mm and 0.18 mm, respectively. The material of the workpiece is Ti6Al4V alloy extensively used for the manufacture of aerospace and medical components.

5.1. Model calibration

First the calibration of the etching rate function has to be performed. In the theory, only one trench is necessary for calibration purposes. However, in practice the measured profile varies due to the fluctuations of the pump pressure and the process noise. In order to avoid this limitation several trenches are generated using the same conditions and an experimental profile is measured from each set of data. Then the average of the different

[4] www.waterjet-group.com

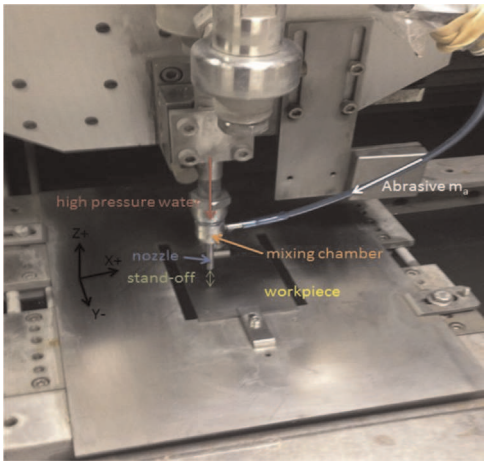

Fig. 3. Experimental setup.

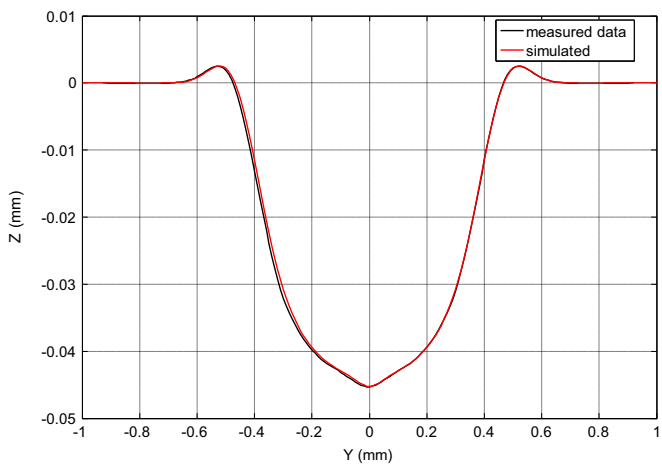

Fig. 4. Average profile used for the calibration and simulated one after calibration.

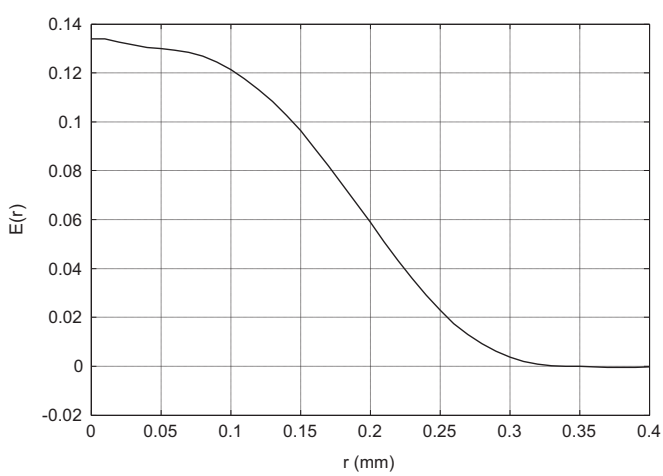

Fig. 5. Etching rate function, E(r).

profiles is calculated. Each trench is generated by moving the jet at 3000 mm/min in the x-direction and the average of the profile in the y-direction is calculated. In Fig. 4 the average profile is displayed. Then using (4) the etching rate function can be calculated (Fig. 5). Once the etching rate function is known the process is simulated using (3) and a simulated profile is obtained (Fig. 4).

Eq. (4) provides a set of points for the etching rate function. For simulation purposes these points are fitted to an equation. The summation of different sinusoidal functions has been found as the

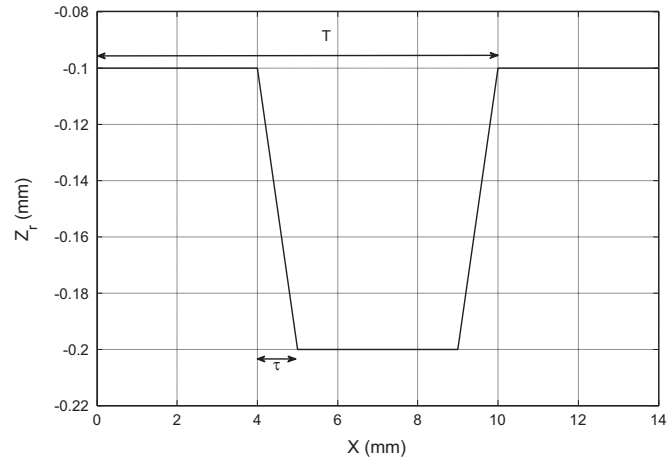

Fig. 6. Target surface.

equation with the best fitting. The etching rate function in Fig. 4 can be fitted to

$$E(r)=\sum_{k=1}^{8} a_k \sin(b_k r+c_k) \tag{13}$$

with $a_1=0.1053$; $b_1=5.916$; $c_1=0.798$; $a_2=0.05573$; $b_2=11.8$; $c_2=1.609$; $a_3=0.003392$; $b_3=33.39$; $c_3=2.911$; $a_4=0.003818$; $b_4=24.07$; $c_4=3.201$; $a_5=0.00117$; $b_5=50.84$; $c_5=1.917$; $a_6=0.001062$; $b_6=60.79$; $c_6=2.325$; $a_7=0.0006665$; $b_7=71.68$; $c_7=2.633$; $a_8=0.0003799$; $b_8=83.96$; $c_8=2.788$.

5.2. Frequency domain analysis

In order to show how the frequency domain analysis is used to select the target surface, the profile described in Fig. 6 is considered. T describes the period of the trapezoidal wave and τ defines the length of the ramp. Small values of τ lead to larger values of the slope and higher frequency components. In Fig. 7a frequency analysis is done for three different values of τ. $\tau=0.25$ mm (red line) leads to larger values of the high frequency modes. These modes are attenuated for $\tau=1$ mm. The Fourier transform of the etching rate function calculated in the previous section is also displayed (dotted black line). The component of the mode of the etching rate function at $f=3\ \mathrm{mm}^{-1}$ is almost zero. This means that the inclusion of this mode in the target surface would lead to a large value of that mode in the trajectory of the beam. Obviously this is not a good idea and any frequency larger than $3\ \mathrm{mm}^{-1}$

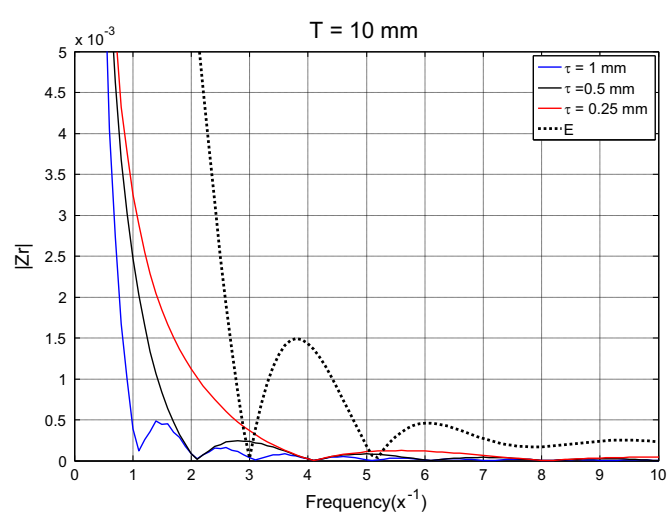

Fig. 7. Target surfaces and etching rate function in the frequency domain.

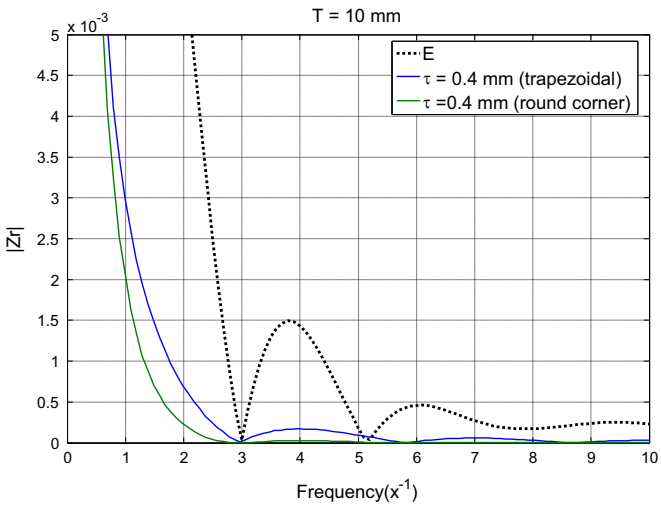

Fig. 8. Final target surface.

should be avoided in the trajectory. In particular, target surfaces with $\tau=1$ mm (blue line in Fig. 7) and $\tau=0.5$ mm (black line in Fig. 7) have a nonzero component at $f=3\ \mathrm{mm}^{-1}$. The solution of the inverse problem for these two profiles would lead to large components around that frequency and undesirable oscillations of the jet.

The target surface is selected in such a way that all the frequency components can be etched by the etching rate function. First τ is selected in such a way that the first minimum is at $f=3\ \mathrm{mm}^{-1}$, which happens when τ is 0.4 mm (blue line in Fig. 8). Moreover, round corners can also be used to filter the high frequencies while the value of the slope of the ramp is kept constant (green line). Finally, the inverse Fourier transform is used to obtain the target profile in the spatial domain, $Z_r(x)$.

5.3. Compensating the dynamics of the machine

In order to show how the dynamics of the machine are compensated, a particular step described as in Fig. 2 is considered, with $Z_1=0.06$ mm and $Z_2=0.12$ mm. These depths are obtained with feed speeds $F_1=3280$ mm/min and $F_2=1640$ mm/min, respectively. Fig. 9 shows the measured value of the gradient of the feed speed in the middle of the step as a function of ΔX. The experiment is performed for both accelerating (red line) and decelerating cases (blue). Positive ($x+$) and negative ($x-$) movements in x-axis of the machine are considered as well. The results show

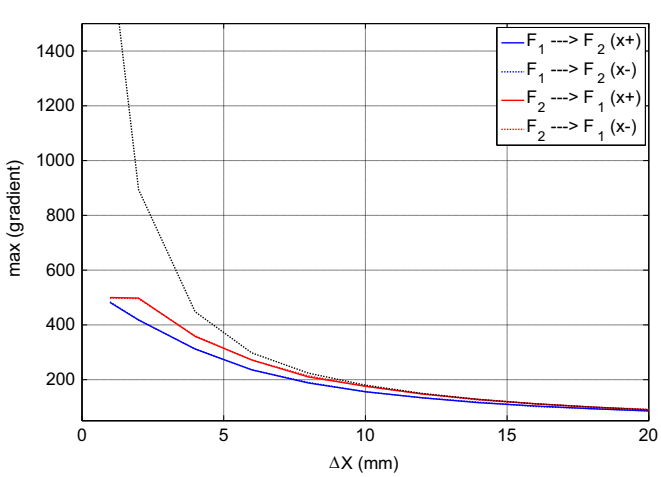

Fig. 9. Maximum gradient calculated in the middle of the step.

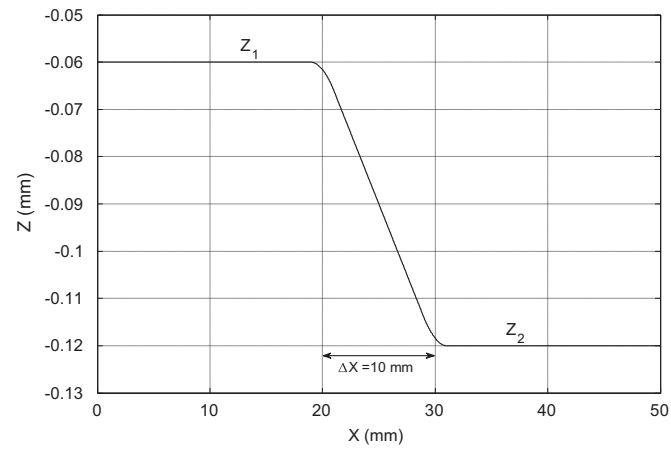

Fig. 10. Target step.

that there is no difference between the positive (solid line) and the negative (dotted line) axis for the same step. However, the value of the gradient achieved is higher when the machine is decelerating. This is an important aspect to be taken into account since most surfaces are etched using raster paths.

Fig. 10 shows a target surface with $Z_1=-0.06$ mm, $Z_2=-0.12$ mm and $\Delta X=10$ mm. The desired value of the slope at the middle of the step is obtained when the gradient of the speed is 184.5 min^{-1}. Now from the results in Fig. 8 that particular value of the gradient is achieved when $\Delta x=7.5$ mm. Moreover, the look-ahead option is compensated by delaying the step 4 mm. Fig. 11 shows the correction of the trajectory. The red line is the compensated trajectory used to generate the input CNC and the black line is the actual measured trajectory of the beam. One can see that the error between the desired trajectory (blue) and the actual trajectory (black) is reduced, while the desired slope in the middle of the step is achieved.

5.4. AWJ milling tests for the linear inverse problem

The target profile is displayed in Fig. 12. Three different values of the depths are considered. The profile is selected by analysing its Fourier transform and checking that all the frequency components can be included. Then the dynamics of the machine are compensated using the technique described above. In Fig. 13a comparison between the measured trajectory after the compensation and the target one is displayed.

The trajectory is implemented in a milling process and the

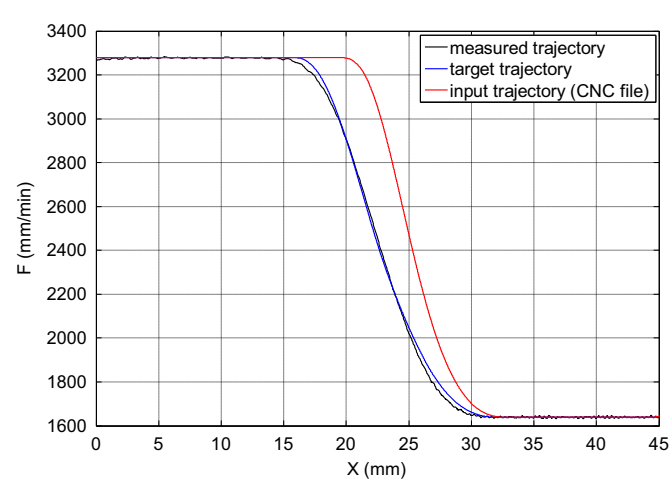

Fig. 11. Target, measured and input trajectories.

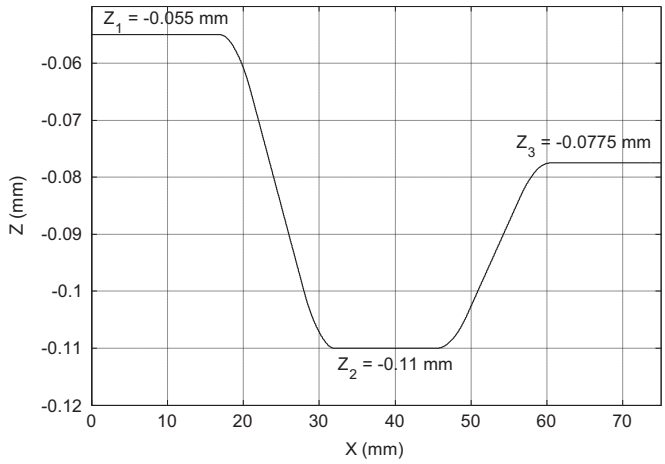

Fig. 12. Target profile.

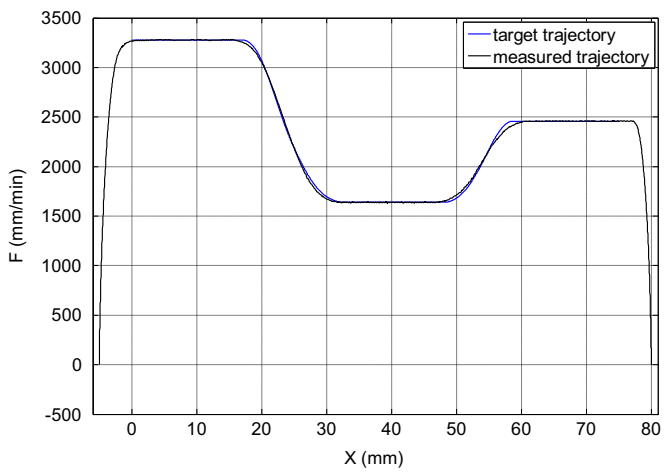

Fig. 13. Target and measured trajectories.

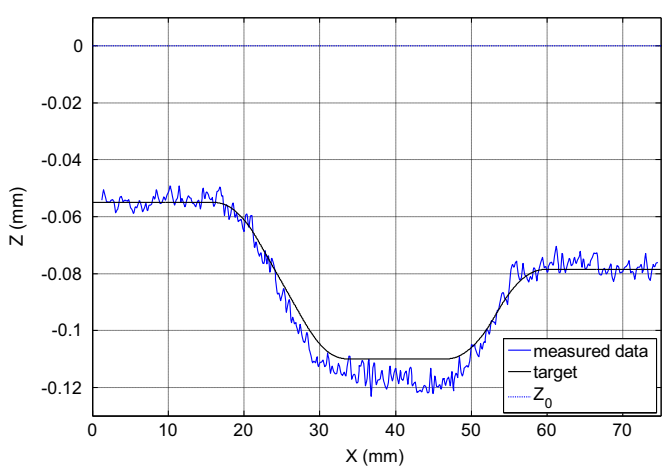

Fig. 14. Target profile and measured data.

profile is measured. Fig. 14 compares the measured profile (blue) and the desired one (black). The tracking error is almost zero for two of the target depths, while there is a small error in the deepest one. Nonlinear effects have more influence at larger depths, since the angle between the jet and the etched surface is larger. Moreover, the measured values of the slopes of both ramps are also close to the target values.

Finally, in order to investigate the limitations of the assumption of linearity, the same trajectory is repeated and the trenches allowed to overlap. Overlapping describes the distance between two consecutive passes in the y-direction (ΔY). Three different overlapping values are considered: $\Delta Y = 0.5$ mm (0%), $\Delta Y = 0.4$ mm (20%) and $\Delta Y = 0.3$ mm (40%), represented by Sections I, II and III, respectively in Fig. 15. Figs. 16–18 show the average profiles in the y-direction for the part of the trajectory with constant speed (and hence constant depth). Sections A, B and C correspond to the constant feed speed parts equal to 3763 mm/min (blue lines), 2503 mm/min (black lines) and 1576 mm/min (red lines), respectively. In Figs. 16–19, the experimental data is displayed with solid lines, while dotted lines are used for the model prediction. Now the nonlinear effect is more evident. For small overlapping, the prediction of the model is still good. However, if the overlapping is large, the linear model is not accurate enough to predict the profile. Moreover, for the same overlapping value the tracking error is always lower for the highest value of the speed, since the resulting profile is shallower and the linear model therefore more accurate. Note that the etched experimental profiles are not constant for the same input parameters. The main reason is that the value of the pressure delivered by the pump used to generate the waterjet is not constant during the process and introduces some noise on the etched surface. We observed that the pressure changed by about 10% around the command input during the experiments. AWJ are usually designed to be used for cutting, where these fluctuations are not so important. However, this value is not so high in general and the noise should be smaller with a better pump.

Experimental tests have shown that the linear model can be used when the etched surface is shallow and the angle between the jet and the surface is approximately constant. However, for deeper surfaces the linear model cannot be used if the surface needs to be etched in one single pass. The best option in that case is to etch the target surface in several passes, where each of these passes only removes a small amount of material and the linear model can be applied. Fig. 19 shows the result of performing two equal passes for the same case described in Section 5.3. The prediction is still good enough for small values of the overlapping.

6. Conclusions

In this paper a new approach to the 1D linear inverse problem for energy beam processes has been presented, with particular emphasis on its application to Abrasive Water Jet milling. A linear model can be used to describe the behaviour of the machine when the angle between the jet and the surface is approximately constant during the whole process and the feed speed is high enough that the etched surface is shallow. Under these conditions a frequency analysis shows that there are fundamental limitations on the frequency content of surfaces that can be milled. These limitations come both from the frequency content of the footprint of the jet and also from the dynamics of the machine. By an appropriate choice of the modes to be included in the target surface, one can ensure that there is a solution of the inverse problem. This is an important result, because this problem is usually solved without considering if there is a solution. Moreover, undesired modes can be filtered and undesirable oscillations in the trajectory of the jet avoided.

The influence of the dynamics of the machine has also been studied. The real trajectory of the jet is always different to the commanded one due to the controller and the limitations of the machine. The precise details of the controller are not known to the user in most devices. In this paper an approach for the compensation of the dynamics for a step in the profile is presented. The value of the slope of the ramp depends on the magnitude of the spatial gradient of the speed of the jet that can be achieved in

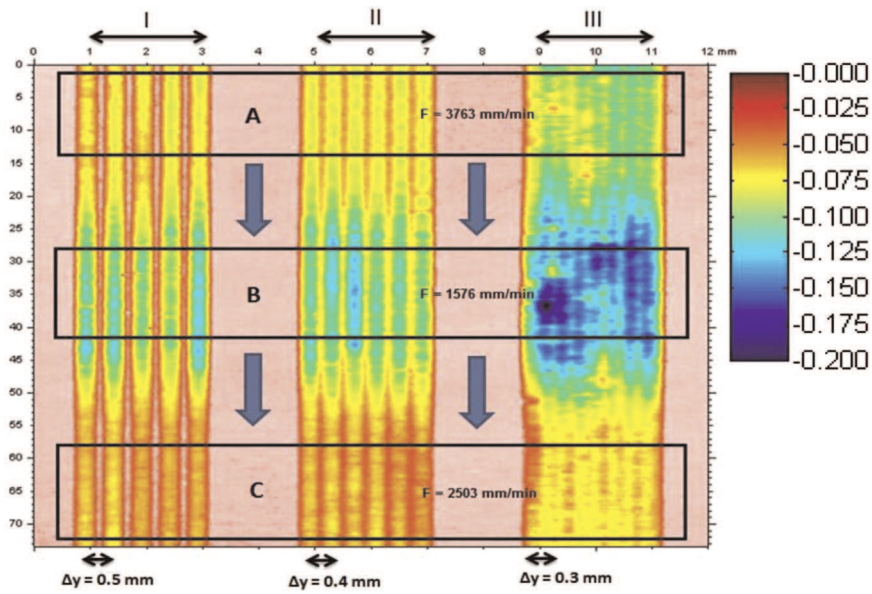

Fig. 15. Measured surface obtained for 3 overlapping values.

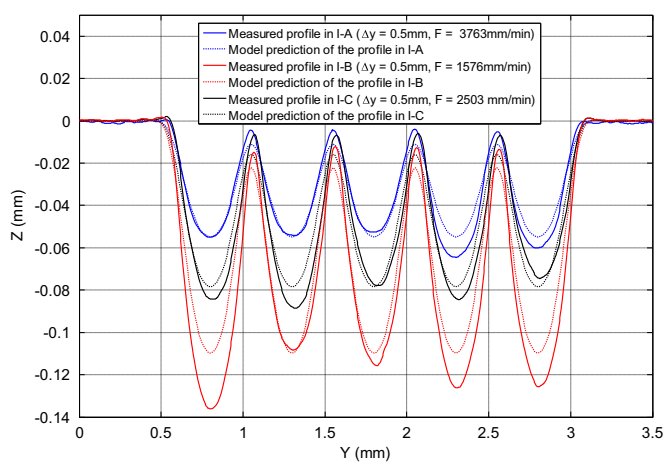

Fig. 16. Average profiles in Section I (Δy=0.5 mm).

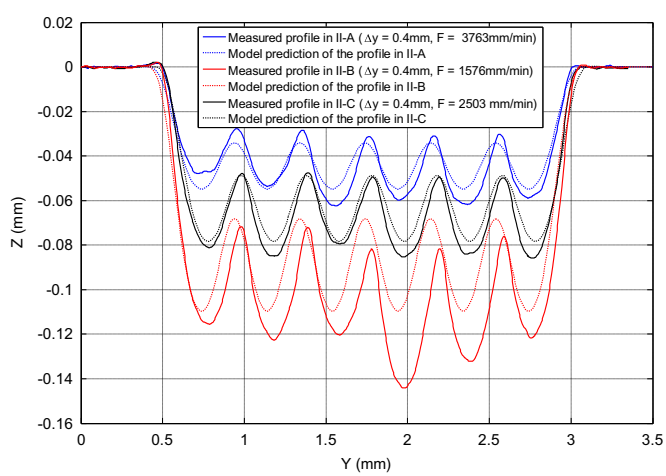

Fig. 17. Average profiles in Section II (Δy=0.4 mm).

practice. Using this information the trajectory is corrected and the error between the desired path and the real one is minimized.

Finally, experimental tests to validate this approach to the inverse problem have been performed. For shallow trenches the

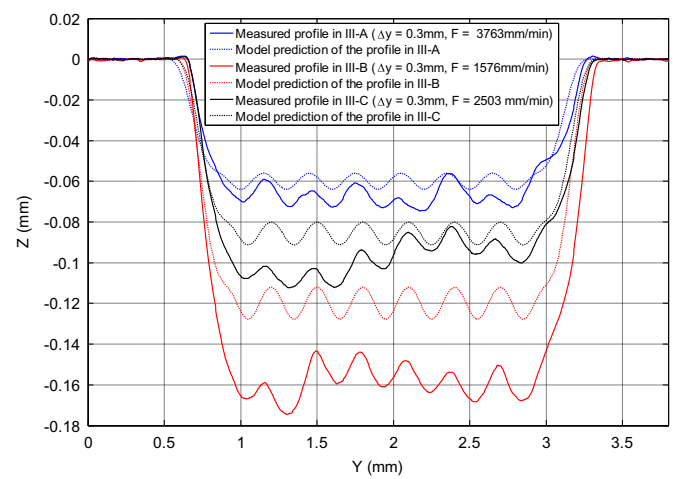

Fig. 18. Average profiles in Section III (Δy=0.3 mm).

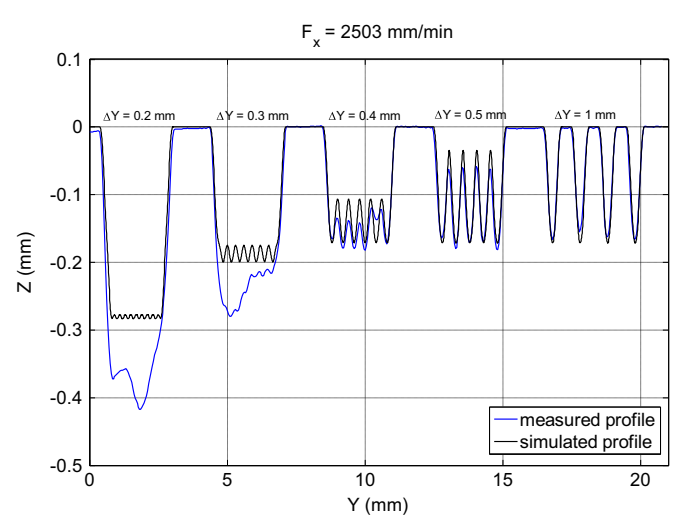

Fig. 19. Examples for average profiles for two passes at F=2503 mm/min and different overlapping values.

tracking error is small, showing that the linear model is quite accurate. For deeper profiles, nonlinear effects are more evident because the angle cannot be considered constant and a nonlinear model should be used. Similarly, the predicted profile is close to the experimental profile when small values of the overlapping are used. Nonlinear effects will form the subject of a future paper. The influence of the fluctuations of the pressure has been observed as well. This is an important aspect and it is being studied in the research group. It will be included as an additional noise in the nonlinear model to be used in the future.

Acknowledgments

The authors would like to acknowledge the funding support of EPSRC project EP/K02826X/1. The authors are also grateful for help and support in the experimental work from Mr. Pablo Lozano of the University of Nottingham. Thanks also go to Mr. Walter Maurer of WaterJet A.G. Switzerland for loaning the AWJ machine for the duration of the project.

References

[1] C. Narayanan, R. Balz, D.A. Weiss, K.C. Heiniger, Modelling of abrasive particle energy in water jet machining, J. Mater. Process. Technol. 213 (12) (2013) 2201–2210.
[2] A.W. Momber, R.R. Kovacevic, Principles of Abrasive Water Jet Machining, Springer-Verlag, London, 1998.
[3] D.S. Miller, Micromachining with abrasive waterjets, J. Mater. Process. Technol. 149 (1–3) (2004) 37–42.
[4] D. Axinte, B. Karpuschewski, M.C. Kong, A.T. Beaucamp, S. Anwar, D. Miller, M. Petzel, High Energy Fluid Jet Machining (HEFJet-Mach): from scientific and technological advances to niche industrial applications, CIRP Ann.-Manuf. Technol. 63 (2) (2014) 751–771.
[5] D.S. Srinivasu, D. Axinte, P.H. Shipway, J. Folkes, Influence of kinematic operating parameters on kerf geometry in abrasive waterjet machining of silicon carbide ceramics, Int. J. Mach. Tools Manuf. 49 (14) (2009) 1077–1088.
[6] L. Ma, R.H. Bao, Y.M. Guo, Waterjet penetration simulation by hybrid code of SPH and FEA, Int. J. Impact Eng. 35/9 (2008) 1035–1042.
[7] Y. Wang, Finite element model of erosive wear on ductile and brittle materials, Wear 265/5-6 (2008) 871–881.
[8] S. Anwar, D. Axinte, A.A. Becker, Finite element modelling of abrasive waterjet milled footprints, J. Mater. Process. Technol. 213 (2) (2013) 180–193.
[9] S. Anwar, D. Axinte, A.A. Becker, Finite element modelling of overlapping abrasive waterjet milled footprints, Wear 303 (1–2) (2013) 426–436.
[10] R. Kovacevic, M. Fang, Modelling of the influence of the abrasive waterjet cutting parameters on the depth of cut based on fuzzy rules, Int. J. Mach. Tools Manuf. 34 (1) (1994) 55–72.
[11] T. Boonkkamp, An analytical solution for etching of glass by powder blasting, J. Eng. Math. 43 (2002) 385–399.
[12] A. Ghobeity, J.K. Spelt, M. Papini, Abrasive jet micro-machining of planar areas of transitional slopes, J. Micromech. Microeng. 18 (5) (2008) 1–13.
[13] D. Axinte, D.S. Srinivasu, J. Billingham, M. Cooper, Geometrical modelling of abrasive waterjet footprints: a study for 90° jet impact angle, Ann. CIRP 59 (1) (2010) 341–346.
[14] M.C. Kong, S. Anwar, J. Billingham, D. Axinte, Mathematical modelling of abrasive waterjet footprints for arbitrarily moving jets: Part I-single straight paths, Int. J. Mach. Tools Manuf. 53 (1) (2012) 58–68.
[15] J. Billingham, C.B. Miron, D.A. Axinte, M.C. Kong, Mathematical modelling of abrasive waterjet footprints for arbitrarily moving jets: Part II-Overlapped single and multiple straight paths, Int. J. Mach. Tools Manuf. 68 (2013) 30–39.
[16] D.P. Adamsa, M.J. Vasile, Accurate focused ion beam sculpting of silicon using a variable pixel dwell time approach, J. Vacuum Sci. Technol. B 24 (2) (2006) 836–844.
[17] P. Domanowski, Inverse problem of shaping by electrochemical generating machining, J. Mater. Process. Technol. 109 (3) (2001) 347–353.
[18] M. Kunieda, Reverse simulation of sinking EDM applicable to large curvatures, Precis. Eng. 36 (2) (2012) 238–243.
[19] J. Madariaga, A. Rabani, D. Axinte, An approach for using iterative learning for controlling the jet penetration depth in abrasive waterjet milling, Int. J. Comput. Integ. Manuf. (2015), In preparation.